ACS APPLIED MATERIALS & INTERFACES

Research Article

www.acsami.org

Rare Earth Complex as Electron Trapper and Energy Transfer Ladder for Efficient Red Iridium Complex Based Electroluminescent Devices

Liang Zhou,* Leijiao Li, Yunlong Jiang, Rongzhen Cui, Yanan Li, Xuesen Zhao, and Hongjie Zhang*

State Key Laboratory of Rare Earth Resource Utilization, Changchun Institute of Applied Chemistry, Chinese Academy of Sciences, Changchun 130022, People's Republic of China

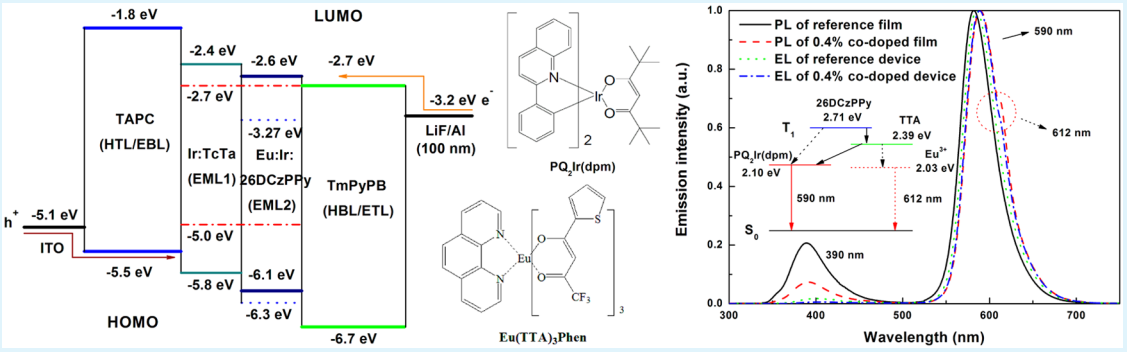

ABSTRACT: In this work, we experimentally demonstrated the new functions of trivalent rare earth complex in improving the electroluminescent (EL) performances of iridium complex by codoping trace $Eu(TTA)_3phen$ (TTA = thenoyltrifluoroacetone, phen = 1,10-phenanthroline) into a light-emitting layer based on $PQ_2Ir(dpm)$ (iridium(III)bis(2-phenylquinoly-*N*,$C^{2'}$)-dipivaloylmethane). Compared with a reference device, the codoped devices displayed higher efficiencies, slower efficiency roll-off, higher brightness, and even better color purity. Experimental results demonstrated that $Eu(TTA)_3phen$ molecules function as electron trappers due to its low-lying energy levels, which are helpful in balancing holes and electrons and in broadening recombination zone. In addition, the matched triplet energy of $Eu(TTA)_3phen$ is instrumental in facilitating energy transfer from host to emitter. Finally, highly efficient red EL devices with the highest current efficiency, power efficiency and brightness up to 58.98 cd A^{-1} (external quantum efficiency (EQE) of 21%), 61.73 lm W^{-1} and 100870 cd m^{-2}, respectively, were obtained by appropriately decreasing the doping concentration of iridium complex. At certain brightness of 1000 cd m^{-2}, EL current efficiency up to 51.94 cd A^{-1} (EQE = 18.5%) was retained. Our investigation extends the application of rare earth complexes in EL devices and provides a chance to improve the device performances.

KEYWORDS: *iridium complex, rare earth complex, electroluminescence, recombination zone, carrier trapping, energy transfer*

INTRODUCTION

Since the demonstration of electroluminescence (EL) originated from triplet excited state, transition metal complexes have been extensively investigated due to their potential application in organic light-emitting devices (OLEDs).[1−4] Both singlet and triplet excitons can be harvested by transition metal complexes, therefore, 100% internal quantum efficiency was expected. Among these complexes, iridium^{III} (Ir^{III}) complexes are most interesting because of their high phosphorescent efficiencies and relatively short excited state lifetimes.[5−7] In recent decades, many groups have given attention to the design of Ir^{III} complexes and the optimization of device structures.[8−12] Significant enhancement of the maximum electroluminescent (EL) efficiencies has been achieved, but the EL efficiencies of most reported devices drop rapidly with increasing current density due to triplet−triplet annihilation, triplet−polaron annihilation, and electric field induced dissociation of excitons.[13,14] The efficiency roll-off is quite severe in phosphorescent OLEDs, and it detrimentally degrades the device performances for practical applications particularly at high brightness.

Recently, Che et al. have reported the significantly improved EL performances of red platinum^{II} (Pt^{II}) complex realized by codoping wide energy gap Ir^{III} complex into electron dominant light-emitting layer (EML) as electron trapper and energy transfer ladder.[15] Experimental results revealed that the codoped Ir^{III} complexes are helpful in balancing the carriers' distribution, broadening the recombination zone, and facilitating the energy transfer from host to emitter because of their low-lying LUMO levels and matched triplet energies. Consequently, the codoped devices displayed significantly improved EL performances. On the basis of the optimization of codoping concentration, highly efficient pure red OLEDs with current efficiency and power efficiency as high as 20.43 cd A^{-1} and 18.33 lm W^{-1}, respectively, were obtained. Even at the

Received: May 19, 2015
Accepted: July 6, 2015
Published: July 15, 2015

DOI: 10.1021/acsami.5b04348
ACS Appl. Mater. Interfaces 2015, 7, 16046−16053

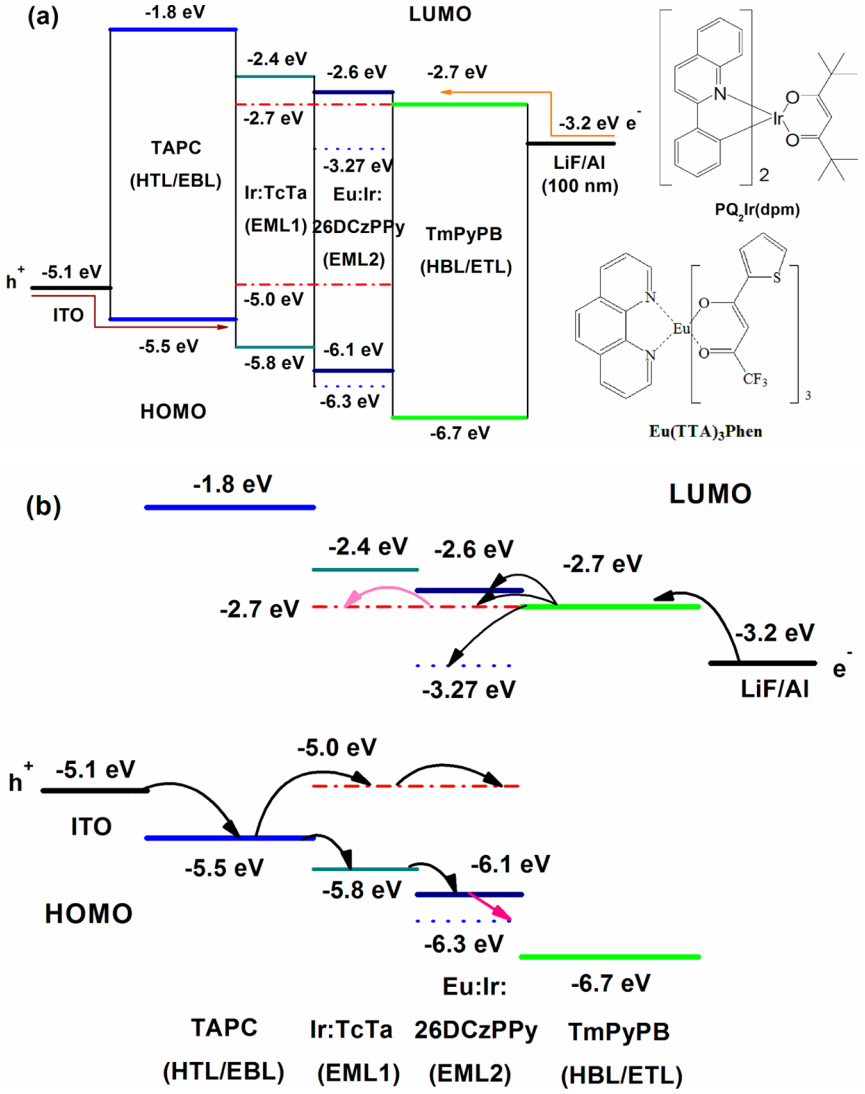

Figure 1. (a) Proposed energy level diagram of the devices used in this work and the molecular structures of $PQ_2Ir(dpm)$ and $Eu(TTA)_3phen$. Within EMLs, the dash dot and dot lines represent the energy levels of $PQ_2Ir(dpm)$ and $Eu(TTA)_3phen$, respectively. (b) Injection and transport processes of holes and electrons in the designed codoped devices.

high brightness of 1000 cd m^{-2}, a high current efficiency of 14.69 cd A^{-1} could be retained.

Alternatively, the relatively cheaper trivalent rare earth complexes have once attracted great interest throughout the world, owing to their highly monochromatic emission and theoretically 100% internal quantum efficiency.[16−19] Previously, much important effort has been paid to doping rare earth complexes into host materials due to their poor carriers' transporting ability and poor film-forming ability.[20,21] However, the low-lying highest occupied molecular orbital (HOMO) and lowest unoccupied molecular orbital (LUMO) levels of most rare earth complexes make it difficult to choose proper host materials.[22,23] Consequently, electrons and holes are generally the majority carriers on rare earth complexes and host materials, respectively. Finally, the complicated carriers' distribution within EML strongly influences the EL processes, and even causes the conversion of dominant EL mechanism.[24,25] In addition, the long excited state lifetimes of rare earth complexes often cause the saturation of excitons particularly at high current density; therefore, a high density of triplet excitons results in severe triplet−triplet annihilation, thus the rapid efficiency roll-off.[26]

In this work, the well-known wide band gap trivalent europium complex $Eu(TTA)_3phen$ (TTA = thenoyltrifluoroacetone, phen = 1,10-phenanthroline) was selected as sensitizer and minutely codoped into electron dominant EML of the double-EMLs devices based on red Ir^{III} complex iridium(III) bis(2-phenylquinoly-$N,C^{2'}$)dipivaloylmethane ($PQ_2Ir(dpm)$) due to its relatively low-lying energy levels.[23,27] Experimental results demonstrated that the codoped $Eu(TTA)_3phen$ molecules act as electron trappers and energy transfer ladders. Compared with the reference device, the $Eu(TTA)_3phen$ codoped devices displayed higher EL efficiencies, slower efficiency roll-off, higher brightness, and even higher color purity attributed to improved carriers' balance, wider recombination zone, and faster energy transfer between host and emitter molecules. More interestingly, the lower doping concentration of $PQ_2Ir(dpm)$ was needed by the codoped devices due to their wider recombination zone and faster energy transfer. By optimizing the concentrations of $Eu(TTA)_3phen$ and $PQ_2Ir(dpm)$, an efficient red EL device

DOI: 10.1021/acsami.5b04348
ACS Appl. Mater. Interfaces 2015, 7, 16046−16053

with the highest current efficiency, power efficiency, and brightness up to 58.98 cd A^{-1} (external quantum efficiency (EQE) of 21%), 61.73 lm W^{-1} and 100 870 cd m^{-2}, respectively, has been obtained. A current efficiency as high as 51.94 cd A^{-1} (EQE = 18.5%) was retained at the certain brightness of 1000 cd m^{-2}.

EXPERIMENTAL SECTION

Materials. All the organic materials used in this study were obtained commercially and used as received, whereas Eu(TTA)$_3$phen was synthesized and purified in our laboratory.

Fabrication of OLEDs. Indium−tin−oxide (ITO) coated glass with a sheet resistance of 10 Ω sq^{-1} was used as the anode substrate. Prior to film deposition, patterned ITO substrates were cleaned with detergent, rinsed in deionized water, dried in an oven, and finally treated with oxygen plasma for 5 min at a pressure of 10 Pa to enhance the surface work function of ITO anode (from 4.7 to 5.1 eV).[28] All of the organic layers were deposited with the rate of 0.1 nm s^{-1} under high vacuum ($\lesssim 2 \times 10^{-5}$ Pa). The doped and codoped layers were prepared by coevaporating dopant(s) and host material from two or three individual sources, and the doping concentrations were modulated by controlling the evaporation rates of dopant(s). MoO_3, LiF, and Al were deposited in another vacuum chamber ($\lesssim 8.0 \times 10^{-5}$ Pa) with the rates of 0.01 and 1 nm s^{-1}, respectively, without being exposed to the atmosphere. The thicknesses of these deposited layers and the evaporation rate of individual materials were monitored in vacuum with quartz crystal monitors. A shadow mask was used to define the cathode and to make ten 10 mm^2 devices on each substrate.

Measurements. Current density−voltage−brightness (J−V−B) characteristics were measured by using a programmable Keithley source measurement unit (Keithley 2400 and Keithley 2000) with a silicon photodiode. The EL spectra were measured with a calibrated Hitachi F−7000 fluorescence spectrophotometer. On the basis of the uncorrected EL fluorescence spectra, the Commission Internationale de l'Eclairage (CIE) coordinates were calculated using the test program of Spectrascan PR650 spectrophotometer. The EQE of EL devices were calculated based on the photo energy measured by the photodiode, the EL spectrum, and the current pass through the device.[29]

RESULTS AND DISCUSSION

The device structure and HOMO/LUMO levels diagram of the designed OLEDs are depicted in Figure 1(a). Due to the high hole mobility (1×10^{-2} cm^2 V^{-1} s^{-1}) and high-lying LUMO level (−1.8 eV), di-[4-(*N*,*N*-ditolyl-amino)-phenyl]cyclohexane (TAPC) was used as hole transport and electron block layers (HTL/EBL).[30] 1,3,5-Tri(*m*-pyrid-3-yl-phenyl)benzene (TmPyPB), which possesses the low-lying HOMO level (−6.7 eV) and high electron mobility (1×10^{-3} cm^2 V^{-1} s^{-1}), was used as hole block/electron transport layer (HBL/ETL).[31] The host materials of EML1 and EML2 were p-type material 4,4′,4″-tris(carbazole-9-yl)triphenylamine (TcTa) and n-type material 2,6-bis(3-(9*H*-carbazol-9-yl)phenyl)pyridine (26DCzPPy), respectively.[31,32] A widely used red Ir^{III} complex PQ_2Ir(dpm) was doped into EMLs as emitter, while the typical europium complex Eu(TTA)$_3$phen was codoped into electron dominant EML2 as sensitizer.[23,27] The molecular structures of Eu(TTA)$_3$phen and PQ_2Ir(dpm) were also shown in Figure 1(a). In this case, the HOMO and LUMO levels (−5.0 and −2.7 eV, respectively) of PQ_2Ir(dpm) are within those of TcTa and 26DCzPPy;[27] therefore, carrier trapping will be the dominant EL mechanism of these devices.[23,33]

According to the previous reports, the stepwise HOMO levels of TAPC (−5.5 eV), TcTa (−5.7 eV), and 26DCzPPy (−6.1 eV) are helpful in facilitating the injection and transport of holes,[30−35] while the stepwise LUMO levels of TmPyPB (−2.7 eV), 26DCzPPy (−2.6 eV), and TcTa (−2.4 eV) are helpful in facilitating the injection and transport of electrons.[31−35] Therefore, balanced carriers' distribution and wide recombination zone were expected. More importantly, the LUMO level of TAPC is 0.6 eV higher than that of TcTa, while the HOMO level of TmPyPB is 0.6 eV lower than that of 26DCzPPy; thus, holes and electrons would be well confined within EMLs.[34,35] Within EML2, electrons will be first trapped by Eu(TTA)$_3$phen molecules due to its lower LUMO level (−3.27 eV) than that of PQ_2Ir(dpm) (−2.7 eV); however, holes would be well trapped by PQ_2Ir(dpm) molecules due to its higher HOMO level (−5.0 eV) than that of 26DCzPPy (−6.1 eV). However, the transfer of holes from TcTa or 26DCzPPy to Eu(TTA)$_3$phen molecules will be insignificant because the HOMO level (−6.3 eV) of Eu(TTA)$_3$phen is even 0.2 eV lower than that of 26DCzPPy (−6.1 eV).

To optimize the doping concentration of PQ_2Ir(dpm), a series of double-EMLs devices with the structure of ITO/TAPC (40 nm)/PQ_2Ir(dpm) (x wt %):TcTa (10 nm)/PQ_2Ir(dpm) (x wt %):26DCzPPy (10 nm)/TmPyPB (40 nm)/LiF (1 nm)/Al (100 nm) was first fabricated and investigated. Where ITO substrate (−5.1 eV) with low-pressure oxygen plasma treatment was utilized as the anode. Experimental results displayed that 4 wt % is the optimal concentration, as listed in Table 1, the 4 wt % doped device (defined as reference device (RD)) achieved the maximal brightness, current efficiency, and power efficiency up to 73 993 cd m^{-2}, 43.34 cd A^{-1} (EQE = 15.4%), and 36.65 lm W^{-1}, respectively. The turn-on voltage ($V_{turn\text{-}on}$, which was defined as the voltage on which the brightness of 1 cd m^{-2} was obtained) of RD is 3.3 V. At an operation voltage of 5.2 V, RD obtained the certain brightness of 1000 cd m^{-2} with the current efficiency up to 40.44 cd A^{-1} (EQE = 14.4%).

Table 1. Key Performances of Co-doped Devices with Eu(TTA)$_3$phen at Different Co-doping Concentrations

device	$V_{turn\text{-}on}$ (V)	B^a (cd m^{-2})	$\eta_c{}^b$ (cd A^{-1})	$\eta_p{}^c$ (lm W^{-1})	η_c (cd A^{-1})^d (1000 cd m^{-2})
0%	3.3	73 993	43.34	36.65	40.44 (5.2 V)
0.2%	3.3	85 315	53.67	46.18	46.60 (5.1 V)
0.4%	3.4	91 109	56.02	48.93	49.72 (5.0 V)
0.6%	3.4	85 345	49.43	43.02	45.22 (5.0 V)

^{a}The data for maximum brightness (B). ^{b}Maximum current efficiency (η_c). ^{c}Maximum power efficiency (η_p). ^{d}Current efficiency (η_c) at the certain brightness of 1000 cd m^{-2}.

Then, three codoped devices with the structure of ITO/TAPC (40 nm)/PQ_2Ir(dpm) (4 wt %):TcTa (10 nm)/Eu(TTA)$_3$phen (y wt %): PQ_2Ir(dpm) (4 wt %):26DCzPPy (10 nm)/TmPyPB (40 nm)/LiF (1 nm)/Al (100 nm) were fabricated and investigated by controlling the concentrations of Eu(TTA)$_3$phen to be 0.2, 0.4, and 0.6 wt %, respectively. With increasing concentration of the codopant Eu(TTA)$_3$phen, as shown in Figure 2(a), EL efficiency increased to a maximum and then decreased gradually. As listed in Table 1, the highest brightness, current efficiency, and power efficiency up to 91 109 cd m^{-2}, 56.02 cd A^{-1} (EQE = 19.9%), and 48.93 lm W^{-1}, respectively, were obtained by the 0.4 wt % codoped device. The same device retained the EL efficiency as high as 49.72 cd A^{-1} (EQE = 17.7%), which was 22.9% higher than that of RD, at the certain brightness of 1000 cd m^{-2} (5.0 V). EL spectra of these codoped devices operating at 5 mA cm^{-2} are given in

DOI: 10.1021/acsami.5b04348
ACS Appl. Mater. Interfaces 2015, 7, 16046−16053

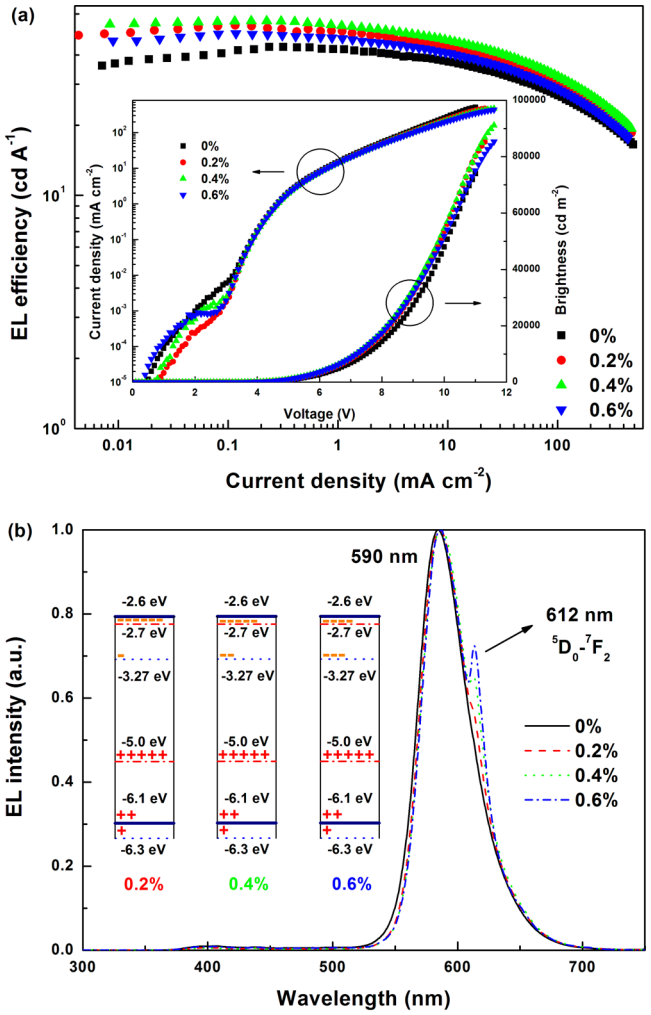

Figure 2. (a) The EL efficiency-current density (η–J) curves of the devices with Eu(TTA)$_3$phen at different codoping concentrations. Insert: Brightness–current density–voltage (B–J–V) characteristics of the devices with Eu(TTA)$_3$phen at different codoping concentrations. (b) Normalized EL spectra of the devices with Eu(TTA)$_3$phen at different codoping concentrations operating at the current density of 5 mA cm^{-2}. Insert: Schematic representation of carriers' distribution within EML2 of the devices with Eu(TTA)$_3$phen at different codoping concentrations. Symbols − and + represent electrons and holes, respectively.

Figure 2(b). Apart from the characteristic emission (590 nm) of PQ$_2$Ir(dpm), these codoped devices displayed the weak emission (612 nm) of Eu(TTA)$_3$phen. The intensity of 612 nm emission increases monotonously with increasing codoping concentration of Eu(TTA)$_3$phen because more and more electrons were trapped by Eu(TTA)$_3$phen molecules within EML2 (as discribed in the inset of Figure 2(b)).

With increasing current density, it is interesting to find the relative density of Eu(TTA)$_3$phen emission in the codoped devices decreased gradually. When the current density is higher than 100 mA cm^{-2}, as shown in Figure 3, no marked Eu(TTA)$_3$phen emission was observed in the 0.4 wt % codoped device. This phenomenon can be interpretated as the saturation of holes and electrons on Eu(TTA)$_3$phen molecules (as shown in the inset of Figure 3) due to the long excited state lifetime and low codoping concentration of Eu(TTA)$_3$phen.[26] Even at very high current density of 300 mA

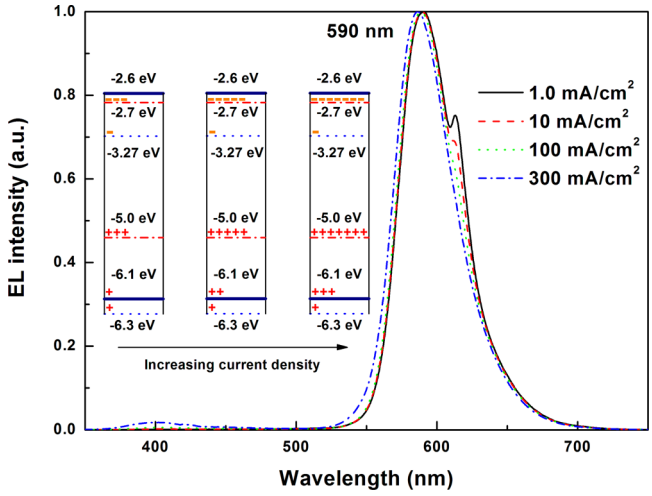

Figure 3. Normalized EL spectra of the 0.4 wt % codoped device operating at different current densities. Insert: Schematic representation of carriers' distribution within EML2 of the 0.4 wt % codoped device operating at different current densities. Symbols − and + represent electrons and holes, respectively.

cm^{-2}, only weak 26DCzPPy emission was observed.[15,35] Correspondingly, the Commission Internationale de l'Eclairage (CIE) coordinates change gradually from (0.59, 0.39) at 1 mA cm^{-2} to (0.57, 0.42) at 300 mA cm^{-2}. These experimental results demonstrated the efficacy of this device design strategy in improving EL performances of OLEDs.

To examine the EL mechanisms of these codoped devices, injection and transport processes of holes and electrons were first investigated. According to our previous investigation,[15] as shown in Figure 1(b), holes will be injected from anode into EML1 via HTL, and some holes could be injected into EML2 through hopping of holes among PQ$_2$Ir(dpm) molecules. Alternatively, electrons will be injected from cathode into EML2 via HBL/ETL, and some electrons could be injected into EML1 through electron hopping among PQ$_2$Ir(dpm) molecules. The LUMO level (−3.27 eV) of Eu(TTA)$_3$phen is 0.57 eV lower than that of PQ$_2$Ir(dpm) (−2.7 eV), which means the codoped Eu(TTA)$_3$phen molecules in EML2 will function as a deeper electron trapper. Consequently, electrons within EML2 will first be trapped by the codoped Eu(TTA)$_3$phen molecules, while holes in both EMLs could be well trapped by PQ$_2$Ir(dpm) molecules due to its higher HOMO level. In this case, the emergence of 26DCzPPy emission demonstrated that some holes and electrons recombine on 26DCzPPy molecules, which means that the transfer of holes from TcTa to 26DCzPPy molecules is still possible. The undiscernable Eu(TTA)$_3$phen emission in EL spectra suggested that few holes and electrons recombine on Eu(TTA)$_3$phen molecules, which confirms that the transfer of holes from 26DCzPPy to Eu(TTA)$_3$phen molecules is very difficult.

To make the improvement mechanisms of EL performances in these codoped devices clear, carriers' distributions in RD and in the codoped double-EMLs devices were analyzed in detail. For RD, as shown in Figure 4, holes and electrons would be the major carriers in EML1 and EML2, respectively, which causes the unbalanced carriers' distribution on PQ$_2$Ir(dpm) molecules within both EMLs. However, for the codoped double-EMLs devices, most holes were trapped by PQ$_2$Ir(dpm) molecules, while some electrons within EML2 will be trapped by

DOI: 10.1021/acsami.5b04348
ACS Appl. Mater. Interfaces 2015, 7, 16046−16053

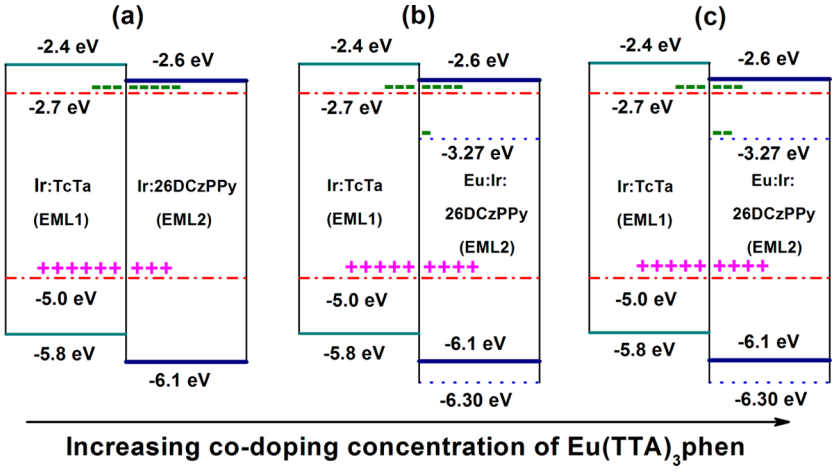

Figure 4. Schematic diagram showing carriers' distribution within the EMLs of RD (a), 0.4% codoped device (b), and 0.6% codoped device (c). The dash dot and dot lines represent the energy levels of $PQ_2Ir(dpm)$ and $Eu(TTA)_3phen$, respectively. Symbols − and + represent electrons and holes, respectively.

$Eu(TTA)_3phen$ molecules. Within EML2, more and more electrons were trapped by $Eu(TTA)_3phen$ molecules with increasing codoping concentration, leading to the decreased electrons on $PQ_2Ir(dpm)$ molecules. Theoretically speaking, improved balance of holes and electrons on $PQ_2Ir(dpm)$ molecules within EML2 could be realized if the codoping concentration of $Eu(TTA)_3phen$ was well optimized. Therefore, the improved balance of holes and electrons on emitter molecules accounts for the significant enhancement of EL efficiency in the $Eu(TTA)_3phen$ codoped devices.

Within EML2, as has been previously discussed,[15] it is difficult for electrons to hop between $Eu(TTA)_3phen$ molecules due to its low doping concentration. However, the transport of electrons through 26DCzPPy molecules is slow because most electrons will be trapped by $PQ_2Ir(dpm)$ and $Eu(TTA)_3phen$ molecules. In other words, the dominant electron transport mechanism within EML2 would be electron hopping between $PQ_2Ir(dpm)$ molecules. Therefore, the codoping of $Eu(TTA)_3phen$ into EML2 would reduce the amount of electrons trapped by $PQ_2Ir(dpm)$ molecules, thus delaying the transport of electrons within EML2 because electron mobility is proportional to the density of electrons involved in the transport process.

To confirm this proposition, electron-only devices with the structure of ITO/TmPyPB (30 nm)/$Eu(TTA)_3phen$ (z wt %):$PQ_2Ir(dpm)$ (4 wt %):26DCzPPy (50 nm)/TmPyPB (30 nm)/LiF (1 nm)/Al (100 nm) were designed. In this case, TmPyPB functions as a hole blocker and electron transporter at the anode and cathode, respectively; therefore, only electrons would be transported in these devices. Four devices were fabricated and examined by controlling the doping concentrations of $Eu(TTA)_3phen$ to be 0, 0.2, 0.4, and 0.6 wt %, respectively. As shown in Figure 5, current density−voltage curve shifted monotonously toward high voltage with increasing $Eu(TTA)_3phen$ doping concentration, which demonstrates the delay of electron transport. In this case, most holes and electrons recombine near the interface between EML1 and EML2. As shown in the inset of Figure 5, the delay of electron transport will shift the recombination center toward cathode, thus broadening the recombination zone. Consequently, the wider recombination zone cause the significant decrease of exciton density, which helps to mitigate the annihilation of excitons and thus delay the roll-off of EL efficiency.

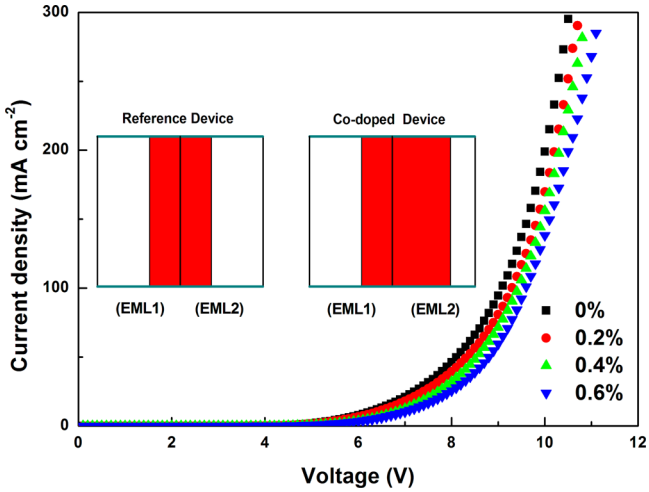

Figure 5. Current density−voltage (J−V) characteristics of the electron-only devices with $Eu(TTA)_3phen$ at different doping concentrations. Insert: Schematic representation of relative recombination zones in reference and codoped devices.

Furthermore, we have also examined the photophysical properties of these codoped systems. The PL spectrum of 50 nm 4 wt % $PQ_2Ir(dpm)$ and 0.4 wt % $Eu(TTA)_3phen$ codoped 26DCzPPy film was compared with that of the 50 nm 4 wt % $PQ_2Ir(dpm)$ doped 26DCzPPy reference film. As shown in Figure 6, the codoped film showed weaker 26DCzPPy emission compared with the reference film. In addition, the EL spectra of RD and the 0.4 wt % $Eu(TTA)_3phen$ codoped device operating at the current density of 100 mA cm^{-2} were also compared in Figure 6. RD displayed weak 26DCzPPy emission, while the 0.4 wt % codoped device displayed undiscernable 26DCzPPy emission. These results altogether revealed that the codoped $Eu(TTA)_3phen$ molecules function as the ladders of energy transfer, thus facilitating the energy transfer from 26DCzPPy to $PQ_2Ir(dpm)$. As shown in the inset of Figure 6, this is supported by the matched triplet energy of the ligand TTA (2.39 eV), which is 0.29 eV higher than that of $PQ_2Ir(dpm)$ (2.10 eV) and is 0.32 eV lower than that of 26DCzPPy (2.71

DOI: 10.1021/acsami.5b04348
ACS Appl. Mater. Interfaces 2015, 7, 16046−16053

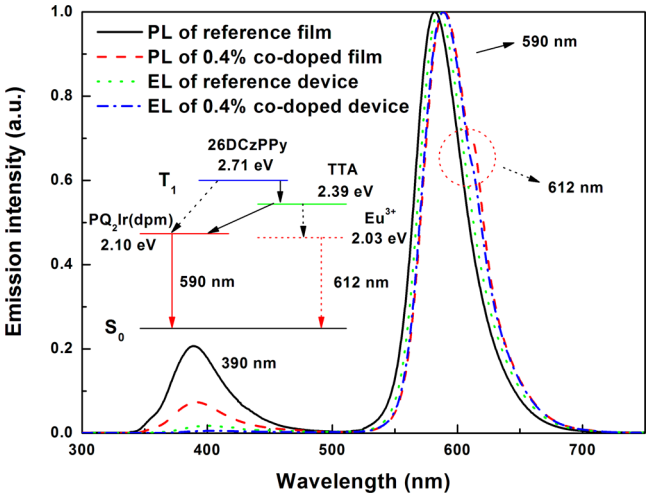

Figure 6. PL spectra of reference and 0.4 wt % codoped films, EL spectra of reference device and 0.4 wt % codoped devices operating at the current density of 10 mA cm^{-2}. Insert: Schematic representation of energy transfer processes from 26DCzPPY to $PQ_2Ir(dpm)$ with $Eu(TTA)_3phen$ as the ladder.

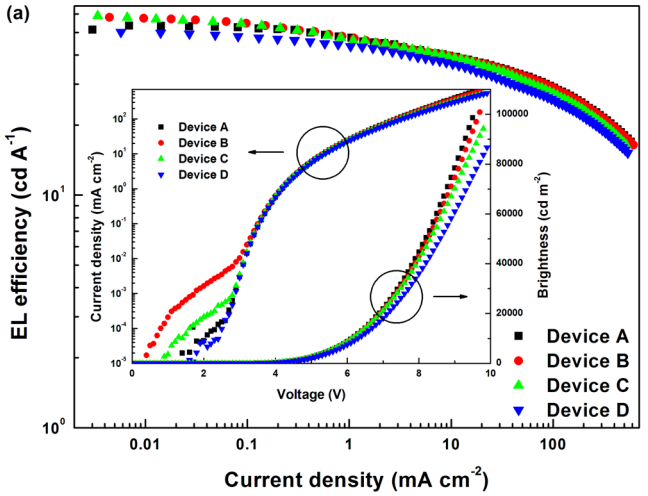

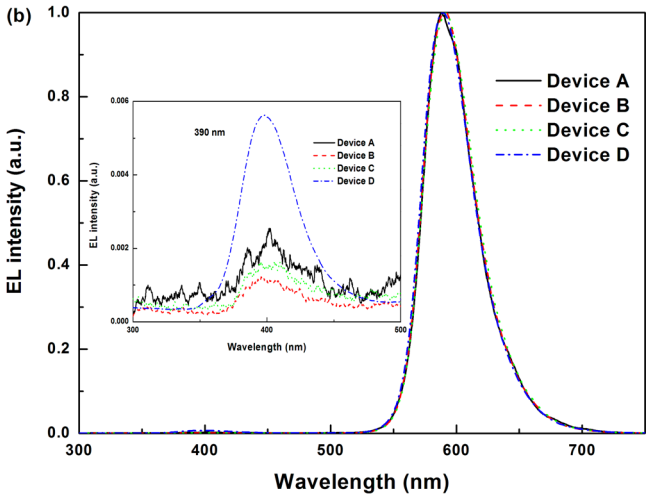

Figure 7. (a) The EL efficiency–current density (η–J) curves of devices A, B, C, and D. Insert: Brightness–current density–voltage (B–J–V) characteristics of devices A, B, C, and D. (b) Normalized EL spectra of devices A, B, C, and D operating at the current density of 200 mA cm^{-2}. Insert: Comparison of 26DCzPPy emission intensity in devices A, B, C, and D.

eV).[26,27,36] Consequently, the improved energy transfer from host to dopant helps to harvest exciton energy particularly at high current density, thus improving the color purity and delaying the roll-off of EL efficiency.

On the basis of the 0.4 wt % $Eu(TTA)_3phen$ codoped device mentioned above, another device (here defined as Device A) was fabricated by incorporating 3 nm MoO_3 anode modified layer between ITO anode and HTL to facilitate the injection of holes.[37−39] Compared with RD, as shown in Figure 7(a) and Table 2, device A displayed lower $V_{turn\text{-}on}$ and operation voltage. Although the maximum current efficiency decreased to 53.52 cd A^{-1} (EQE = 19.0%), device A obtained the higher maximum power efficiency of 54.21 lm W^{-1} due to the lower operation voltage, thus achieving a maximum brightness of 98 627 cd m^{-2}. At the brightness of 1000 cd m^{-2} (4.5 V), this device retained the EL efficiency as high as 48.92 cd A^{-1} (EQE = 17.4%), which was 21.0% higher than that of RD.

With a broadening recombination zone of holes and electrons, theoretically speaking, more and more emitter molecules will participate in EL processes,[40] thus decreasing the needed concentration of the emitter. By keeping the doping concentration of $Eu(TTA)_3phen$ constant at 0.4%, three codoped devices were fabricated, decreasing the doping concentration of $PQ_2Ir(dpm)$ to be 3.5 wt % (Device B), 3.0 wt % (Device C), and 2.5 wt % (Device D), respectively. With a decreasing doping concentration of $PQ_2Ir(dpm)$, as shown in Figure 7(a), both current density–voltage curve and brightness–voltage curve shifted gradually toward high voltage, while EL efficiency increased gradually to a maximum at 3.0% and then decreased rapidly. As listed in Table 2, the highest EL current efficiency and power efficiency of 58.98 cd A^{-1} (EQE = 21.0%) and 61.73 lm W^{-1}, respectively, were obtained by device C, while the highest brightness of 100 870 cd m^{-2} was realized by device B due to its slower efficiency roll-off. Even at the certain brightness of 1000 cd m^{-2} (4.5 V), device B can retain the current efficiency up to 51.94 cd A^{-1} (EQE = 18.5%), which was 28.4% higher than that of RD. Interestingly, as shown in Figure 7(b), 26DCzPPy emission decreases first and then increases gradually with a decreasing doping concentration of $PQ_2Ir(dpm)$. Among these devices, device B displayed the best color purity. These results demonstrate the lower needed doping concentration of $PQ_2Ir(dpm)$ in $Eu(TTA)_3phen$ codoped devices attributed to the broadening of recombination zone.

Table 2. Key Performances of Devices A, B, C, and D

device	$V_{turn\text{-}on}$ (V)	B^a (cd m^{-2})	$\eta_c{}^b$ (cd A^{-1})	$\eta_p{}^c$ (lm W^{-1})	η_c (cd A^{-1})^d (1000 cd m^{-2})
A	3.0	98 627	53.52	54.21	48.92 (4.5 V)
B	3.0	100 870	58.08	60.79	51.94 (4.5 V)
C	3.0	94 229	58.98	61.73	47.84 (4.5 V)
D	3.1	86 722	50.22	50.86	44.33 (4.6 V)

^{a}The data for maximum brightness (B). ^{b}Maximum current efficiency (η_c). ^{c}Maximum power efficiency (η_p). ^{d}Current efficiency (η_c) at the certain brightness of 1000 cd m^{-2}.

CONCLUSIONS

In summary, we have demonstrated an efficient device design strategy by codoping low-lying energy levels rare earth complex $Eu(TTA)_3phen$ into an electron dominant EML. Experimental results revealed that the codoped $Eu(TTA)_3phen$ molecules

DOI: 10.1021/acsami.5b04348
ACS Appl. Mater. Interfaces 2015, 7, 16046−16053

function as deeper electron trappers, thus causing the broadening of the recombination zone as well as facilitating the balance of holes and electrons on the emitter molecules. Due to the matched triplet energies of 26DCzPPy, Eu(TTA)$_3$phen, and PQ$_2$Ir(dpm), the codoped Eu(TTA)$_3$phen molecules also function as the energy transfer ladders between 26DCzPPy and PQ$_2$Ir(dpm). Compared with the control device, the Eu(TTA)$_3$phen codoped devices displayed significantly improved EL performances. Furthermore, the codoping of Eu(TTA)$_3$phen molecules decreased the needed doping concentration of PQ$_2$Ir(dpm). The optimized codoped device exhibited the maximum EL current efficiency, power efficiency, and brightness up to 58.98 cd A^{-1} (EQE = 21.0%), 61.73 lm W^{-1}, and 100 870 cd m^{-2}, respectively. At a certain brightness of 1000 cd m^{-2}, the current efficiency up to 51.94 cd A^{-1} (EQE = 18.5%) was retained.

AUTHOR INFORMATION

Corresponding Authors

*Tel.: +8643185262127; fax: +8643185685653; e-mail: zhoul@ciac.ac.cn (L.Z.).

*Tel.: +8643185262127; fax: +8643185685653; e-mail: hongjie@ciac.ac.cn (H.Z.).

Notes

The authors declare no competing financial interest.

ACKNOWLEDGMENTS

The authors thank Professor Youxuan Zheng for helpful discussions. The authors are grateful for the financial aid from National Natural Science Foundation of China (Grant Nos. 21201161, 51402286, 91122030, 21210001, and 21221061), National Key Basic Research Program of China (No. 2014CB643802), Youth Innovation Promotion Association CAS (2013150), and Jilin Provincial Science and Technology Development Program of China (20130522125JH).

REFERENCES

(1) Ma, Y.; Zhang, H.; Shen, J.; Che, C.-M. Electroluminescence from Triplet Metal-Ligand Charge-Transfer Excited State of Transition Metal Complexes. *Synth. Met.* **1998**, *94*, 245−248.

(2) Baldo, M. A.; O'Brien, D. F.; You, Y.; Shoustikov, A.; Sibley, S.; Thompson, M. E.; Forrest, S. R. Highly Efficient Phosphorescent Emission from Organic Electroluminescent Devices. *Nature* **1998**, *395*, 151−154.

(3) Yang, X.; Wang, Z.; Madakuni, S.; Li, J.; Jabbour, G. E. Efficient Blue- and White-Emitting Electrophosphorescent Devices Based on Platinum(II) [1,3-Difluoro-4,6-di(2-pyridinyl)benzene] Chloride. *Adv. Mater.* **2008**, *20*, 2405−2409.

(4) Seino, Y.; Sasabe, H.; Pu, Y.-J.; Kido, J. High-Performance Blue Phosphorescent OLEDs Using Energy Transfer from Exciplex. *Adv. Mater.* **2014**, *26*, 1612−1616.

(5) Jou, J.-H.; Lin, Y.-X.; Peng, S.-H.; Li, C.-J.; Yang, Y.-M.; Chin, C.-L.; Shyue, J.-J.; Sun, S.-S.; Lee, M.; Chen, C.-T.; Liu, M.-C.; Chen, C.-C.; Chen, G.-Y.; Wu, J.-H.; Li, C.-H.; Sung, C.-F.; Lee, M.-J.; Hu, J.-P. Highly Efficient Yellow Organic Light Emitting Diode with a Novel Wet- and Dry-Process Feasible Iridium Complex Emitter. *Adv. Funct. Mater.* **2014**, *24*, 555−562.

(6) Lamansky, S.; Djurovich, P.; Murphy, D.; Abdel-Razzaq, F.; Lee, H. E.; Adachi, C.; Burrows, P. E.; Forrest, S. R.; Thompson, M. E. Highly Phosphorescent Bis-Cyclometalated Iridium Complexes: Synthesis, Photophysical Characterization, and Use in Organic Light Emitting Diodes. *J. Am. Chem. Soc.* **2001**, *123*, 4304−4312.

(7) Wang, Q.; Ding, J. Q.; Ma, D. G.; Cheng, Y. X.; Wang, L. X.; Jing, X. B.; Wang, F. S. Harvesting Excitons Via Two Parallel Channels for Efficient White Organic LEDs with Nearly 100% Internal Quantum Efficiency: Fabrication and Emission-Mechanism Analysis. *Adv. Funct. Mater.* **2009**, *19*, 84−95.

(8) Zhu, Y.-C.; Zhou, L.; Li, H.-Y.; Xu, Q.-L.; Teng, M.-Y.; Zheng, Y.-X.; Zuo, J.-L.; Zhang, H.-J.; You, X.-Z. Highly Efficient Green and Blue-Green Phosphorescent OLEDs Based on Iridium Complexes with the Tetraphenylimidodiphosphinate Ligand. *Adv. Mater.* **2011**, *23*, 4041−4046.

(9) Yang, C.-H.; Cheng, Y.-M.; Chi, Y.; Hsu, C.-J.; Fang, F.-C.; Wong, K.-T.; Chou, P.-T.; Chang, C.-H.; Tsai, M.-H.; Wu, C.-C. Blue-Emitting Heteroleptic Iridium(III) Complexes Suitable for High-Efficiency Phosphorescent OLEDs. *Angew. Chem., Int. Ed.* **2007**, *46*, 2418−2421.

(10) Tao, Y. T.; Wang, Q.; Yang, C. L.; Wang, Q.; Zhang, Z. Q.; Zou, T. T.; Qin, J. G.; Ma, D. G. A Simple Carbazole/Oxadiazole Hybrid Molecule: An Excellent Bipolar Host for Green and Red Phosphorescent OLEDs. *Angew. Chem., Int. Ed.* **2008**, *47*, 8104−8107.

(11) Lee, S.; Shin, H.; Kim, J.-J. High-Efficiency Orange and Tandem White Organic Light-Emitting Diodes Using Phosphorescent Dyes with Horizontally Oriented Emitting Dipoles. *Adv. Mater.* **2014**, *26*, 5864−5868.

(12) Wang, R.; Liu, D.; Ren, H.; Zhang, T.; Yin, H.; Liu, G.; Li, J. Highly Efficient Orange and White Organic Light-Emitting Diodes Based on New Orange Iridium Complexes. *Adv. Mater.* **2011**, *23*, 2823−2827.

(13) Jeon, W. S.; Park, T. J.; Kim, S. Y.; Pode, R.; Jang, J.; Kwon1, J. H. Low Roll-Off Efficiency Green Phosphorescent Organic Light-Emitting Devices with Simple Double Emissive Layer Structure. *Appl. Phys. Lett.* **2008**, *93*, 063303.

(14) Kalinowski, J.; Stampor, W.; Me-zyk, J.; Cocchi, M.; Virgili, D.; Fattori, V.; DiMarco, P. Quenching Effects in Organic Electrophosphorescence. *Phys. Rev. B: Condens. Matter Mater. Phys.* **2002**, *66*, 235321.

(15) Zhou, L.; Kwong, C.-L.; Kwok, C.-C.; Cheng, G.; Zhang, H.; Che, C.-M. Efficient Red Electroluminescent Devices with Sterically Hindered Phosphorescent Platinum(II) Schiff Base Complexes and Iridium Complex Codopant. *Chem. - Asian J.* **2014**, *9*, 2984−2994.

(16) Zhou, L.; Deng, R.; Feng, J.; Li, X.; Li, X.; Zhang, H. Improved Color Purity and Electroluminescent Efficiency Obtained by Modulating Thickness and Evaporation Rates of Hole Block and Electron Transport Layers. *Appl. Surf. Sci.* **2011**, *257*, 3033−3038.

(17) Liang, C. J.; Zhao, D.; Hong, Z. R.; Zhao, D. X.; Liu, X. Y.; Li, W. L.; Peng, J. B.; Yu, J. Q.; Lee, C. S.; Lee, S. T. Improved Performance of Electroluminescent Devices Based on an Europium Complex. *Appl. Phys. Lett.* **2000**, *76*, 67−69.

(18) Kido, J.; Okamot, Y. Organo Lanthanide Metal Complexes for Electroluminescent Materials. *Chem. Rev.* **2002**, *102*, 2357−2368.

(19) Xin, H.; Li, F. Y.; Shi, M.; Bian, Z. Q.; Huang, C. H. Efficient Electroluminescence from a New Terbium Complex. *J. Am. Chem. Soc.* **2003**, *125*, 7166−7167.

(20) Hu, W.; Matsumura, M.; Wang, M.; Jin, L. Efficient Red Electroluminescence From Devices Having Multilayers of a Europium Complex. *Appl. Phys. Lett.* **2000**, *77*, 4271−4273.

(21) Yu, J.; Zhou, L.; Zhang, H.; Zheng, Y.; Li, H.; Deng, R.; Peng, Z.; Li, Z. Efficient Electroluminescence from New Lanthanide (Eu^{3+}, Sm^{3+}) Complexes. *Inorg. Chem.* **2005**, *44*, 1611−1618.

(22) Zhou, L.; Deng, R.; Zhang, H. Suppression of Efficiency Roll-Off in Co-Ddoped Electroluminescent Devices Based on Europium Complex. *Chin. J. Inorg. Chem.* **2014**, *30*, 113−120.

(23) Zhou, L.; Zhang, H. J.; Deng, R. P.; Li, Z. F.; Yu, J. B.; Guo, Z. Y. Conversion Process of the Dominant Electroluminescence Mechanism in a Molecularly Doped Organic Light-Emitting Device With Only Electron Trapping. *J. Appl. Phys.* **2007**, *102*, 064504.

(24) Zhou, L.; Zhang, H. J.; Meng, Q. G.; Liu, F. Y.; Yu, J. B.; Deng, R. P.; Peng, Z. P.; Li, Z. F.; Guo, Z. Y. Change of the Dominant Luminescent Mechanism With Increasing Current Density in Molecularly Doped Organic Light-Emitting Devices. *J. Lumin.* **2007**, *126*, 644−652.

(25) Zhou, L.; Zhang, H. J.; Shi, W. D.; Deng, R. P.; Li, Z. F.; Yu, J. B.; Guo, Z. Y. Mechanisms of Efficiency Enhancement in the Doped

DOI: 10.1021/acsami.5b04348
ACS Appl. Mater. Interfaces 2015, 7, 16046−16053

Electroluminescent Devices Based on a Europium Complex. *J. Appl. Phys.* **2008**, *104*, 114507.
(26) Adachi, C.; Baldo, M. A.; Forrest, S. R. Electroluminescence Mechanisms in Organic Light Emitting Devices Employing a Europium Chelate Doped in a Wide Energy Gap Bipolar Conducting Host. *J. Appl. Phys.* **2000**, *87*, 8049−8055.
(27) D'Andrade, B. W.; Holmes, R. J.; Forrest, S. R. Efficient Organic Electrophosphorescent White-Light-Emitting Device with a Triple Doped Emissive Layer. *Adv. Mater.* **2004**, *16*, 624−628.
(28) Chan, I.-M.; Cheng, W.-C.; Hong, F. C. Enhanced Performance of Organic Light-Emitting Devices by Atmospheric Plasma Treatment of Indium Tin Oxide Surfaces. *Appl. Phys. Lett.* **2002**, *80*, 13−15.
(29) Sun, P. P.; Duan, J. P.; Lih, J. J.; Cheng, C. H. Synthesis of New Europium Complexes and Their Application in Electroluminescent Devices. *Adv. Funct. Mater.* **2003**, *13*, 683−691.
(30) Lee, J.; Chopra, N.; Eom, S.-H.; Zheng, Y.; Xue, J.; So, F.; Shi, J. Effects of Triplet Energies and Transporting Properties of Carrier Transporting Materials on Blue Phosphorescent Organic Light Emitting Devices. *Appl. Phys. Lett.* **2008**, *93*, 123306.
(31) Su, S.-J.; Gonmori, E.; Sasabe, H.; Kido, J. Highly Efficient Organic Blue-and White-Light-Emitting Devices Having a Carrier- and Exciton-Confining Structure for Reduced Efficiency Roll-Off. *Adv. Mater.* **2008**, *20*, 4189−4194.
(32) Ikai, M.; Tokito, S.; Sakamoto, Y.; Suzuki, T.; Taga, Y. Highly Efficient Phosphorescence From Organic Light-Emitting Devices with an Exciton-Block Layer. *Appl. Phys. Lett.* **2001**, *79*, 156−158.
(33) Uchida, M.; Adachi, C.; Koyama, T.; Taniguchi, Y. Charge Carrier Trapping Effect by Luminescent Dopant Molecules in Single-Layer Organic Light Emitting Diodes. *J. Appl. Phys.* **1999**, *86*, 1680−1687.
(34) Parker, I. D. Carrier Tunneling and Device Characteristics in Polymer Light-Emitting Diodes. *J. Appl. Phys.* **1994**, *75*, 1656−1666.
(35) Zhou, L.; Kwok, C.-C.; Cheng, G.; Zhang, H.; Che, C.-M. Efficient Red Organic Electroluminescent Devices by Doping Platinum(II) Schiff Base Emitter into Two Host Materials with Stepwise Energy Levels. *Opt. Lett.* **2013**, *38*, 2373−2375.
(36) Xiao, L.; Chen, Z.; Qu, B.; Luo, J.; Kong, S.; Gong, Q.; Kido, J. Recent Progresses on Materials for Electrophosphorescent Organic Light-Emitting Devices. *Adv. Mater.* **2011**, *23*, 926−952.
(37) Tao, C.; Ruan, S.; Zhang, X.; Xie, G.; Shen, L.; Kong, X.; Dong, W.; Liu, C.; Chen, W. Performance Improvement of Inverted Polymer Solar Cells with Different Top Electrodes by Introducing a MoO_3 Buffer Layer. *Appl. Phys. Lett.* **2008**, *93*, 193307.
(38) Hamwi, S.; Meyer, J.; Winkler, T.; Riedl, T.; Kowalsky, W. *P* -type Doping Efficiency of MoO_3 in Organic Hole Transport Materials. *Appl. Phys. Lett.* **2009**, *94*, 253307.
(39) Kröger, M.; Hamwi, S.; Meyer, J.; Riedl, T.; Kowalsky, W.; Kahn, A. Role of the Deep-Lying Electronic States of MoO_3 in the Enhancement of Hole-Injection in Organic Thin Films. *Appl. Phys. Lett.* **2009**, *95*, 123301.
(40) Kalinowski, J.; Palilis, L. C.; Kim, W. H.; Kafafi, Z. H. Determination of the Width of the Carrier Recombination Zone in Organic Light-Emitting Diodes. *J. Appl. Phys.* **2003**, *94*, 7764−7767.

DOI: 10.1021/acsami.5b04348
ACS Appl. Mater. Interfaces 2015, 7, 16046−16053